

# Solid-State Polymerization Reaction by Combined In-Situ X-ray Diffraction and X-ray Absorption Spectroscopy (XRD–EXAFS)

Matthias Epple,<sup>\*,†,‡</sup> Gopinathan Sankar,<sup>§</sup> and John Meurig Thomas<sup>\*,§,||</sup>

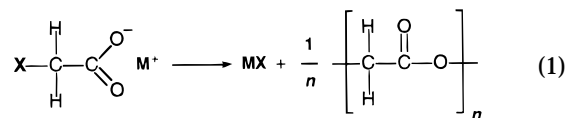
*Institute of Inorganic and Applied Chemistry, University of Hamburg, Martin-Luther-King-Platz 6, D-20146 Hamburg, Germany; Davy Faraday Laboratory, The Royal Institution of Great Britain, 21 Albemarle Street, London W1X 4BS, U.K.*

Received June 12, 1997. Revised Manuscript Received August 12, 1997<sup>®</sup>

The solid-state polymerization reaction of sodium bromoacetate has been studied with combined in situ X-ray diffraction and X-ray absorption spectroscopy (XRD–EXAFS). This elimination reaction leads quantitatively to sodium bromide and poly(hydroxyacetic acid), polyglycolide. Both XRD and EXAFS data have been quantitatively analyzed to yield the molar fractions of educt and products during the reaction. Results of both methods confirm that the reaction is occurring without a crystalline, liquid, or amorphous intermediate in one single step. Sodium bromide is precipitated in small crystals in the polymeric matrix. The growth of the microcrystals could be followed by analyzing the XRD line width during the reaction, an observation that is corroborated by scanning electron microscopy. This allows a control of the pore size distribution of the obtained material by variation of the reaction temperature.

## Introduction

For over 140 years it has been known<sup>1,2</sup> that alkali-metal salts of halogenoacetic acids eliminate alkali halides upon heating and concomitantly undergo a solid-state polymerization—ostensibly without formation of detectable crystalline intermediates—to yield polyglycolide, a polyester that is now of considerable practical value as a biomaterial, especially in medicine. It is used, for example, as a resorbable bone fixation device,<sup>3,4</sup> as an intestinal anastomotic device,<sup>5</sup> or as a surgical suture.<sup>6</sup> In general, such polyhydroxycarboxylic acids are of excellent biocompatibility because of their good biodegradability and nontoxicity (see ref 7 for a recent review). Conventionally, they are prepared either via the corresponding hydroxycarboxylic acids or biotechnologically.<sup>8,9</sup> In contrast to these products, polyglycolide prepared by solid-state reaction has a distinct porous morphology that may be advantageous for application as a biomaterial.<sup>10,11</sup>



It is of interest to inquire, in the context of the mechanisms of solid-state transformations, whether this solid-state reaction proceeds through a well-defined (possibly noncrystalline) intermediate, since it has recently been observed in inorganic systems, such as the conversion of a Mg<sup>2+</sup> ion-exchanged zeolite X to cordierite,<sup>12</sup> and of the recently discovered synthetic titanosilicate JDF-L1<sup>13</sup> to the mineral-phase narsarsuokite.<sup>14</sup> Knowledge of the reaction pathway is indispensable for a rational control over the morphology of the product.

Thermally induced polymerizations in the organic solid state<sup>10,15–20</sup> have been much less intensively investigated than photoinduced oligomerizations and polymerizations.<sup>21–27</sup> In cases of a topochemical control of the reaction, the crystal structure of the parent

<sup>†</sup> University of Hamburg.

<sup>‡</sup> Fax: +49 40/4123-6348. E-mail: epple@xray.chemie.uni-hamburg.de.

<sup>§</sup> The Royal Institution of Great Britain.

<sup>||</sup> Fax: +44 171/6293569.

<sup>®</sup> Abstract published in *Advance ACS Abstracts*, September 15, 1997.

- (1) Hoffmann, R. *Liebigs Ann. Chem.* **1857**, 102, 1.
- (2) Kekulé, A. *Liebigs Ann. Chem.* **1858**, 105, 288.
- (3) Hofmann, G. O. *Arch. Orthop. Trauma Surg.* **1995**, 114, 123.
- (4) Ashammakhi, N.; Rokkanen, P. *Biomaterials* **1997**, 18, 3.
- (5) Wood, J. S.; Frost, D. B. *Am. Surg.* **1993**, 59, 642.
- (6) Ooster, P. J.; Gjøde, P.; Mortensen, B. B.; Bartholin, J.; Gottrup, F. *Br. J. Surg.* **1995**, 82, 1080.
- (7) Chiellini, E.; Solaro, R. *Adv. Mater.* **1996**, 8, 305.
- (8) Kricheldorf, H. R. *Handbook of polymer synthesis*; Marcel Dekker: New York, 1992.
- (9) Kricheldorf, H. R.; Kreiser-Saunders, I. *Macromol. Symp.* **1996**, 103, 85.
- (10) Epple, M.; Tröger, L. *J. Chem. Soc., Dalton Trans.* **1996**, 11.
- (11) Epple, M.; Kirschnick, H. *Chem. Ber.* **1996**, 129, 1123.
- (12) Sankar, G.; Wright, P. A.; Natarajan, S.; Thomas, J. M.; Greaves, G. N.; Dent, A. J.; Dobson, B. R.; Ramsdale, C. A.; Jones, R. H. *J. Phys. Chem.* **1993**, 97, 9550.
- (13) Roberts, M. A.; Sankar, G.; Thomas, J. M.; Jones, R. H.; Du, H.; Chen, J.; Pang, W.; Xu, R. *Nature* **1996**, 381, 401.

(14) Roberts, M. A.; Sankar, G.; Thomas, J. M. Submitted for publication.

(15) Kohlschütter, H. W.; Sprenger, L. *Z. Phys. Chem.* **1932**, B16, 284.

(16) Jakabhazy, S. Z.; Morawetz, H.; Morosoff, N. *J. Polym. Sci. C* **1963**, 4, 805.

(17) Takao, Y.; Kasashima, Y.; Inoki, M.; Akutsu, F.; Naruchi, K.; Yamaguchi, Y. *Polym. J.* **1995**, 27, 766.

(18) Cho, T. H.; Chaudhuri, B.; Snider, B. B.; Foxman, B. M. *J. Chem. Soc., Chem. Commun.* **1996**, 1337.

(19) Schlitter, S. M.; Beck, H. P. *Chem. Ber.* **1996**, 129, 1561.

(20) Epple, M.; Kirschnick, H.; Thomas, J. M. *J. Therm. Anal.* **1996**, 47, 331.

(21) Schmidt, G. M. J. *Pure Appl. Chem.* **1971**, 27, 647.

(22) Thomas, J. M. *Philos. Trans. R. Soc.* **1974**, A277, 251.

(23) Wegner, G. *Pure Appl. Chem.* **1977**, 49, 443.

(24) Thomas, J. M. *Pure Appl. Chem.* **1979**, 51, 1065.

(25) Nakanishi, H.; Jones, W.; Thomas, J. M.; Hasegawa, M. *Proc. R. Soc., Ser. A* **1980**, 369, 307.

(26) Hasegawa, M. *Chem. Rev. (Washington, D.C.)* **1983**, 83, 507.

(27) Enkelmann, V.; Wegner, G. *J. Am. Chem. Soc.* **1993**, 115, 10390.

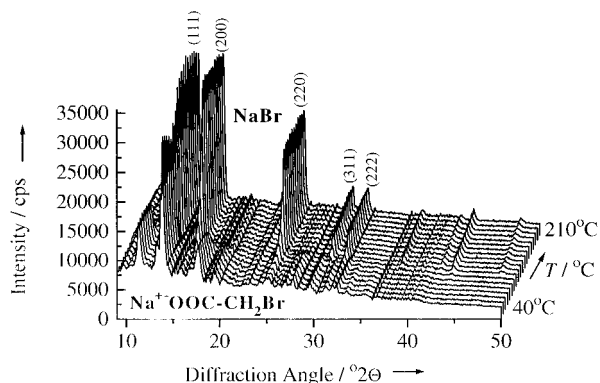


**Figure 1.** X-ray powder diffractograms obtained during heating of sodium bromoacetate. The difference between consecutive scans is 600 s or 9.5 K. The heating rate was 0.95 K min<sup>-1</sup>. The X-ray wavelength was  $\lambda = 0.9193 \text{ \AA}$ .

compound determines the reaction pathway and thereby the product.<sup>21,24</sup> However, it has to be ensured that the reaction proceeds in one step, involving no liquid or amorphous intermediates. In the case of the solid-state reduction reaction of benzophenones,<sup>28</sup> it has recently been shown that temporary liquefaction due to eutectic melting occurs.<sup>29</sup> Such an observation renders all mechanistic considerations based on crystal structures obsolete.

The analogous reaction in sodium chloroacetate has been studied with a number of structure-sensitive techniques.<sup>10,11,20</sup> No intermediate could be detected. However, ex situ studies are often not representative of the true reaction pathway because of possible sample transformations during quenching and storage.<sup>30,31</sup> Furthermore, it is not clear whether the results that were obtained for sodium chloroacetate can be uncritically transposed to sodium bromoacetate. Sodium bromoacetate has been studied in situ by combined simultaneous DSC-EXAFS.<sup>32</sup> The latter technique related enthalpy change and short-range order, but both methods are not as sensitive to other phases as diffraction techniques.

Combined use of two in situ synchrotron radiation-based techniques, X-ray powder diffraction, XRD (which probes long-range crystallographic order), and extended X-ray absorption fine structure (EXAFS), which quantitatively determines the immediate structural environment (short range order) around a specific, selected atom, is an ideally suited double-pronged approach to tackle such problems—see refs 12, 31, and 33–36 for further details. To our knowledge, it has not yet been applied to a reacting molecular solid. This realization, together with the still incomplete knowledge about the reaction pathway, inspired us to study this reaction in situ, thereby relating, by two separate sets of experi-

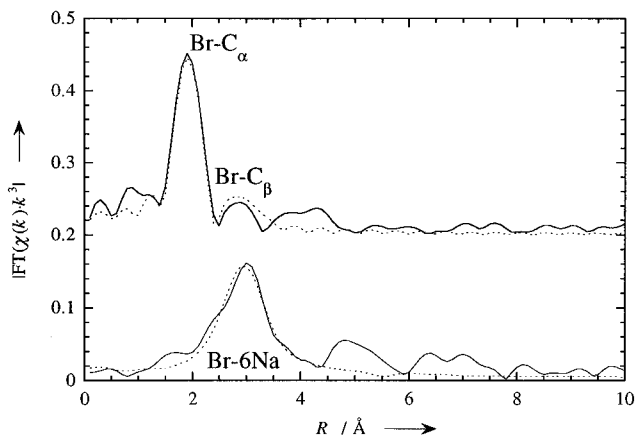
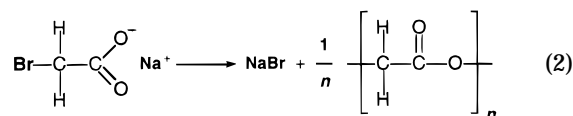


**Figure 2.** Fourier transform magnitudes of sodium bromoacetate (upper graph) and sodium bromide (lower graph), both measured at room temperature. For sodium bromoacetate, two carbon shells were fitted, and for sodium bromide the six next-nearest sodium neighbors. Solid lines represent experimental data, dotted lines theoretical fit curves. The data are corrected for phase shifts.

ments (DSC-EXAFS and XRD-EXAFS), long- and short-range order and enthalpy change. A major goal was the quantitative evaluation of the obtained data in terms of the reaction progress in order to yield a thorough characterization of the reaction.

## Results and Discussion

Armed with the combined in situ tools of XRD and EXAFS described in the references cited earlier, we embarked on a detailed study of sodium bromoacetate that undergoes simultaneous elimination and polymerization when heated to above 100 °C.



The X-ray diffraction patterns clearly show the conversion from sodium bromoacetate to sodium bromide (Figure 1). The reaction occurs rapidly within a few scans. No crystalline intermediates are detectable.

The EXAFS Fourier transforms are strongly different for sodium bromoacetate and sodium bromide (Figure 2). The first carbon neighbor ( $C_\alpha$ ) attached to bromine in sodium bromoacetate gives rise to a strong peak at  $R \approx 1.9 \text{ \AA}$ , and the second carbon neighbor ( $C_\beta$ ) is visible as a smaller peak at  $R \approx 2.8 \text{ \AA}$ . The inorganic reaction product sodium bromide is mainly characterized by the shell of six sodium cations at a distance of  $R \approx 2.9 \text{ \AA}$ . Br- $C_\beta$  shell and Br-Na shell are easily separable because of different backscattering behavior.

Figure 3 shows the magnitude of the Fourier-transformed EXAFS spectra during the reaction. Visual inspection suggests that the transformation occurs without production of detectable intermediates.

To estimate the temperature effects on the experimental results, we first studied a standard NaBr sample by combined XRD-EXAFS while heating it through the same temperature range. We used these data to quantitatively evaluate the EXAFS spectra of the temperature-resolved data of sodium bromoacetate, in particular, by fixing the Debye-Waller factor during the

- (28) Toda, F.; Kiyoshige, K.; Yagi, M. *Angew. Chem.* **1989**, *101*, 329.  
 (29) Epple, M.; Ebbinghaus, S.; Reller, A.; Gloistein, U.; Cammenga, H. K. *Thermochim. Acta* **1995**, *269/270*, 433.  
 (30) Epple, M. *Thermochim. Acta* **1995**, *269/270*, 33.  
 (31) Thomas, J. M.; Thomas, W. J. *Principles and practice of heterogeneous catalysis*; VCH: Weinheim, 1996.  
 (32) Epple, M.; Sazama, U.; Reller, A.; Hilbrandt, N.; Martin, M.; Tröger, L. *J. Chem. Soc., Chem. Commun.* **1996**, 1755.  
 (33) Couves, J. W.; Thomas, J. M.; Waller, D.; Jones, R. H.; Dent, A. J.; Derbyshire, G. E.; Greaves, G. N. *Nature* **1991**, *354*, 465.  
 (34) Clausen, B. S.; Gråbæk, L.; Steffensen, G.; Hansen, P. L.; Topsøe, H. *Catal. Lett.* **1993**, *20*, 23.  
 (35) Thomas, J. M.; Greaves, G. N. *Science* **1994**, *265*, 1675.  
 (36) Thomas, J. M.; Greaves, G. N.; Catlow, C. R. A. *Nucl. Instrum. Methods* **1995**, *B97*, 1.

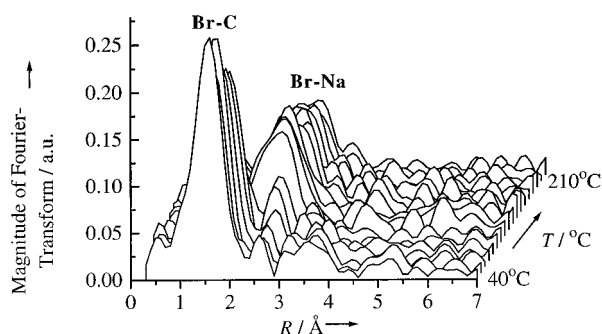


**Figure 3.** Magnitude of Fourier transforms obtained from Br K-edge spectra. The first coordination shell of the educt (sodium bromoacetate) consists of one carbon neighbor, and the first shell in the product (sodium bromide) of six sodium ions. The data are not corrected for phase-shifts.

fits. Details of the fitting parameters are listed in Table 1. The resulting values for  $N(\text{Br}-\text{C}_\omega)$  and  $N(\text{Br}-\text{Na})$  are a direct measure of the extent of reaction  $\alpha$ . The precise value of  $\alpha$  could be computed after normalization to  $N(\text{Br}-\text{C}_\omega)(t=0) = 1$  and  $N(\text{Br}-\text{Na})(t=\infty) = 6$ .

Quantitative evaluation of both EXAFS and XRD results yields the extent of reaction  $\alpha$  (see Figure 4). Both sodium bromoacetate and sodium bromide were monitored with each method so that all four sets of data were obtained. The reaction proceeds rapidly in a narrow temperature interval (ca. 80–120 °C). All data lie on the same  $\alpha/T$  curve. This indicates two important points. First, since the extents of reaction computed for educt and product are equal within the accuracy of our data, no intermediate can have formed; otherwise, there would have been some discrepancy between  $\alpha$  determined from sodium bromoacetate and  $\alpha$  from sodium bromide. Second, the results for  $\alpha$  obtained from EXAFS (probing short-range order) and X-ray diffraction (probing long-range order) are identical. This indicates that no amorphous or liquid intermediate phase is involved in the overall transformation. Such an intermediate, were it present, would give rise to a shift between EXAFS and XRD results. Thus, the solid-state reaction (eq 2) occurs in one step that simultaneously affects short- and long-range order. However, the EXAFS method gives only information about the bromine environment. The formation of the purely organic product, i.e., polyglycolide, cannot be followed by EXAFS. The scattering peaks of the formed polyglycolide are too weak to be quantitatively evaluated.

Every 10 min two data sets (EXAFS and XRD) were measured. The accuracy in  $\alpha$  derived from XRD is around 2.3%. The accuracy in EXAFS is more difficult to estimate owing to possible similarities in the bromine environment between the present phases, but it is estimated to about 10% in  $\alpha$ . Taking into account these limitations, we can conclude that any intermediate, were it present, could have a lifetime of a few minutes at maximum and a maximum concentration of a few percent.

The reason for the decrease in  $\alpha$  above 140 °C is not known. It might be due to some radiation damage suffered by sodium bromide. This would decrease the X-ray diffraction intensity, and it would also increase the static disorder in the bromine environment, causing a higher Debye–Waller factor  $\sigma^2(\text{Br}-\text{Na})$ . Since  $\sigma^2(\text{Br}-\text{Na})$  was kept constant during the fit, the high correlation between  $N(\text{Na})$  and  $\sigma^2(\text{Br}-\text{Na})$  would result in an

(apparently) decreasing coordination number  $N(\text{Na})$ . This assumption is corroborated by the observation that the intensity of the (220) peak in pure NaBr also decreases during the heating program. It should be noted here that all X-ray diffraction intensities were corrected for beam fluctuations by monitoring the incoming beam intensity.

The temperature interval in which the reaction takes place (80–120 °C) is remarkably different from that found in the simultaneous DSC–EXAFS experiment (140–170 °C).<sup>32</sup> The heating rate was almost identical in both experiments (0.95 K min<sup>-1</sup> vs 1.0 K min<sup>-1</sup>), whereas the applied temperature program (40–210 °C vs 120–200 °C) was not. That means that sample X irradiation prior to the reaction was longer in the XRD–EXAFS experiment than in the DSC–EXAFS experiment (about 42 vs 20 min). This could have led to radiation damage of the lattice and thereby an increased reaction rate, since solid-state reactions frequently start at lattice defects.<sup>37,38</sup> In standard DSC experiments, i.e., without any irradiation, the reaction starts at  $186 \pm 10$  °C,<sup>11</sup> a fact that corroborates the above assumption. Another difference between the two experiments was the material used for sample dilution (fumed silica in XRD–EXAFS and boron nitride in DSC–EXAFS) that may not be completely inert under strong irradiation and elevated temperature. This underscores that it is highly advantageous to use simultaneous techniques rather than to subsequently apply single techniques, since sample environment and reaction conditions are never completely the same when employing different methods.

Careful analysis of the X-ray diffractograms revealed that the peak width of the formed sodium bromide decreases with temperature. For the (220) peak at  $25.2^\circ 2\theta$ , the full width at half-maximum (fwhm) decreases from  $0.442^\circ 2\theta$  (95 °C) to  $0.284^\circ 2\theta$  (180 °C). It remains constant thereafter. This indicates that the crystallite size increases with rising temperature. We computed the average crystallite size using the Scherrer equation.<sup>39,40</sup>

The crystallites grow almost linearly with temperature (see Figure 4). It is noteworthy that the growth of the crystallites still continues after the reaction is completed at ca. 120 °C. This points to extensive diffusion in the reacted solid, a remarkable fact given the low reaction temperature. In earlier studies with scanning electron microscopy on the morphology of the formed reaction products, we found that the alkali halide is precipitated in small cubes ( $d \approx 1 \mu\text{m}$ ) in the polymeric matrix.<sup>10,11</sup> The above results are in perfect agreement with these findings, since they demonstrate how the precipitated cubes are growing with time and temperature. Scanning electron microscopy on polyglycolide samples obtained from sodium bromoacetate that had been polymerized at 170, 180, and 190 °C for 100, 60, and 45 min gave average crystallite diameters of 0.3, 0.5, and 0.9  $\mu\text{m}$ , respectively. Keeping in mind the various assumptions in the Scherrer equation,<sup>41</sup> this

(37) Brown, W. E.; Dollimore, D.; Galwey, A. K. *Reactions in the solid state*; Elsevier: Amsterdam, 1980.

(38) Schmalzried, H. *Chemical Kinetics of Solids*; VCH: Weinheim, 1995.

(39) Scherrer, P. *Göttinger Nachr.* **1918**, 2, 98.

(40) Kaelble, E. F. *Handbook of X-rays*; McGraw-Hill: New York, 1967.

**Table 1: Variation of Parameters for the Quantitative Evaluation of Br K-edge EXAFS Spectra of Reacting Sodium Bromoacetate**

compound	shell	$N$	$R/\text{\AA}$	$1000\sigma^2/\text{\AA}^2$	$1000B/\text{\AA}^2$
Br-CH <sub>2</sub> -COONa	Br-C <sub>α</sub>	variable	variable (1.935–1.957)	3.0	0
Br-CH <sub>2</sub> -COONa	Br-C <sub>β</sub>	$N(C_{\beta}) = N(C_{\alpha})$	3.017	8.5	0
NaBr	Br-Na	variable	variable (2.959–2.980)	$4.85 + 0.07125 \times T/K$	$-11.61 + 0.0571 \times T/K$

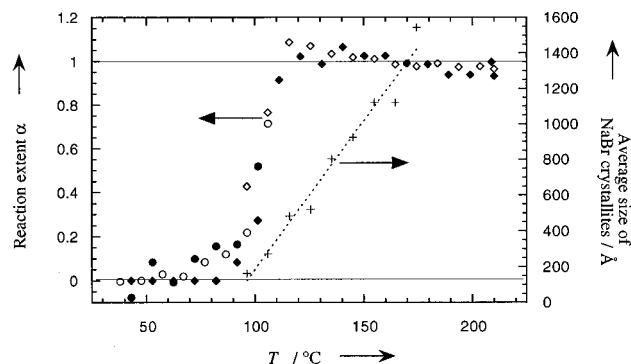


**Figure 4.** Reaction extent  $\alpha$  vs time from X-ray diffractometry and X-ray absorption spectroscopy. Parent and product phase were both detected with each method. All points follow the same trend, therefore no intermediates seem to occur. Additionally, the average size of the sodium bromide crystallites that are formed during the reaction is shown (as derived from XRD). The crystallites grow with an almost linear rate, even after the reaction is chemically finished (at ca. 120 °C). Symbols are defined as follows: ●  $1-N(C_1)$  of sodium bromoacetate by EXAFS; ◆  $N(\text{Na})/6$  of NaBr by EXAFS; ◇  $I(t)/I(t = \infty)$  of the NaBr (220) diffraction peak at 25.2° 2 $\theta$ ; ○,  $1 - I(t)/I(t = 0)$  of the sodium bromoacetate diffraction peak at 11.3° 2 $\theta$ ; +, average NaBr crystallite size (from the width of the NaBr (220) peak).

corresponds well with the results from X-ray diffraction. It should be emphasized that these numbers do not represent equilibrium values for crystallite diameters. It is expected that the crystallites would continue to grow upon further annealing, driven by the need to minimize the interfacial energy.

Summarizing, it can be said that the solid-state polymerization reaction in sodium bromoacetate does not occur through crystalline, liquid, or amorphous intermediates within the experimental detection limit. Thus, a topochemical control of the reaction is very likely. The experiments presented here, together with the data obtained earlier by simultaneous DSC–EXAFS,<sup>32</sup> show that enthalpy and short- and long-range order change simultaneously. Such a quantitative determination of the reaction extent from both EXAFS and XRD is rare.

Unfortunately, the crystal structure of sodium bromoacetate is not known owing to extreme difficulties in obtaining suitable single crystals, a fact generally observed for alkali halogenoacetates. The crystal structures of silver chloroacetate<sup>42</sup> and sodium chloroacetate<sup>43</sup> were obtained recently under considerable difficulties, the former from a single crystal, the latter from synchrotron powder diffraction data. Both crystal structures support a topochemical elimination of AgCl and NaCl, respectively. Figure 5 shows the X-ray powder diffractograms of sodium chloroacetate, sodium bromoacetate, and silver chloroacetate. The diffraction

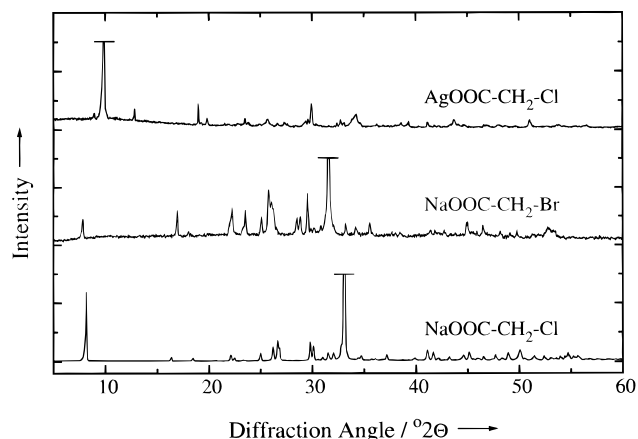


**Figure 5.** Comparison of the X-ray diffraction patterns of sodium chloroacetate, sodium bromoacetate and silver chloroacetate (Cu K $\alpha$  radiation,  $\lambda = 1.5418 \text{\AA}$ ).

patterns are similar, indicating a structural relationship. It was neither possible to grow suitable single crystals of sodium bromoacetate nor to unambiguously index the pattern of sodium bromoacetate.

The growth of the precipitated sodium bromide crystals could be followed in situ. It is remarkable that extensive diffusion of NaBr occurs at very moderate temperatures (100–200 °C). This underscores that reacting solids are highly dynamic systems that must be treated differently from reacting liquids or solutes. A characterization by a single scalar variable, i.e., the reaction extent  $\alpha$ , is by no means sufficient to understand the complex processes involved. In situ techniques are very valuable tools for gaining closer insight into such systems, although no single experiment, even if it is a sophisticated combined one, is capable of revealing all details of the mechanism. Nevertheless, it has been shown that the pore size distribution in the remaining polyglycolide after washing out the NaBr crystallites can be adjusted by choice of the appropriate reaction temperature and time. Higher reaction temperature and longer annealing time both lead to an increase in NaBr crystallite (and thereby pore) size.

## Experimental Section

Sodium bromoacetate was prepared as described in ref 11. Its purity and the absence of sodium bromide were assured by IR, <sup>1</sup>H and <sup>13</sup>C NMR, X-ray powder diffraction and elemental analysis (C, H).

Combined XRD–EXAFS data were collected at station 9.3 at the Daresbury synchrotron laboratory. This station is equipped with instrumentation for simultaneous Quick-EXAFS spectroscopy (“QEXAFS”)<sup>44</sup> and X-ray powder diffraction.<sup>12,45</sup> The storage ring was run in multibunch mode (2 GeV, ca. 200–250 mA). The samples were mixed with fumed silica (4:3 = w/w) and pressed to a pellet that was brought into a custom-made furnace (static air atmosphere). EXAFS data were recorded in transmission mode, and XRD data were recorded with a curved position sensitive detector. The

(41) Bish, D. L.; Post, J. E., Eds.; *Modern powder diffraction*; Mineralogical Society of America: Washington, DC, 1989.

(42) Epple, M.; Kirschnick, H. *Chem. Ber.* **1997**, *130*, 291.

(43) Elizabé, L.; Kariuki, B. M.; Harris, K. D. M.; Tremayne, M.; Epple, M.; Thomas, J. M. *J. Phys. Chem.*, Submitted.

(44) Frahm, R. *Rev. Sci. Instrum.* **1989**, *60*, 2515.

(45) Thomas, J. M.; Greaves, G. N. *Catal. Lett.* **1993**, *20*, 337.

temperature was recorded in the immediate vicinity of the sample with a thermocouple (estimated accuracy of  $\pm 2$  K). X-ray powder diffraction patterns were recorded for 180 s at  $\lambda = 0.9193$  Å followed by a 40 s dead time. Then an X-ray absorption spectrum was taken at the bromine K-edge ( $E \approx 13\,455$  eV) for 380 s (resulting time resolution of 600 s). The sample was heated from 40 to 210 °C at 0.95 K min<sup>-1</sup>. Additionally, EXAFS spectra and X-ray diffractograms of educt and product phases were measured before and after the reaction at room temperature. The extent of reaction of XRD data was obtained by integration and subsequent normalization of the NaBr (220) peak at  $25.2^\circ 2\theta$  and the sodium bromoacetate peak at  $11.3^\circ 2\theta$ . This is permitted because no mass loss occurs during the reaction.<sup>46</sup>

EXAFS data evaluation was carried out using the programs EXCALIB, EXBROOK, and EXCURV92 available at the Daresbury laboratory.<sup>47</sup> All scans were manually corrected for short-time discontinuities ("glitches") before evaluation. All plots and evaluations were done with  $k^3$ -weighted spectra using a  $k$  range of 3–10.5 Å<sup>-1</sup>. EXAFS data were strongly influenced by multiple excitation, a phenomenon well-known for bromine EXAFS.<sup>32,48–50</sup> This was corrected by a simplified procedure.<sup>51</sup>

Quantitative EXAFS analysis was performed as follows. The first shell of six sodium neighbors in the standard NaBr sample was computed using a cumulant expression for the Debye–Waller factor  $\sigma^2$ . The third cumulant  $B$  is defined in

(46) Epple, M. *J. Therm. Anal.* **1995**, *45*, 1265.

(47) Binstedt, N.; Campbell, J. W.; Gurman, S. J.; Stephenson, P. C. *EXCURV92*; SERC Daresbury Laboratory, 1991.

(48) Li, G.; Bridges, F.; Brown, G. S. *Phys. Rev. Lett.* **1992**, *68*, 1609.

(49) D'Angelo, P.; Di Cicco, A.; Filipponi, A.; Pavel, N. V. *Phys. Rev. A* **1993**, *47*, 2055.

(50) Burattini, E.; D'Angelo, P.; Di Cicco, A.; Filipponi, A.; Pavel, N. V. *J. Phys. Chem.* **1993**, *97*, 5486.

(51) Epple, M.; Kirschnick, H.; Greaves, G. N.; Sankar, G.; Thomas, J. M. *J. Chem. Soc., Faraday Trans.* **1996**, *92*, 5035.

the program EXCURV92 as  $B = \frac{4}{3}C_3^3$  with  $C_3$  being the third cumulant of the original EXAFS expression.<sup>47,52–54</sup> A linear expression was fitted for the temperature dependence of  $\sigma^2$  and  $B$ . These values were then used in evaluating the EXAFS spectra of the reacting sodium bromoacetate. The first two carbon shells of sodium bromoacetate were also fitted but without cumulants for the Debye–Waller factor. If higher cumulants were introduced for Br–C shells, they assumed values close to zero, indicating an almost symmetric pair distribution function. The values of  $R$  and  $\sigma^2$  for these two shells were derived from room-temperature EXAFS spectra and found to be constant within the investigated temperature range. The amplitude reduction factor  $s_0^2$  was fixed to 1, and the zero-energy correction  $E_0$  was allowed to vary. The values for  $\sigma^2(\text{Br}-C_n)$  and  $R(\text{Br}-C_n)$  are in good agreement with earlier results for Br–C bonds.<sup>32,50,51</sup>

**Acknowledgment.** M.E. thanks Prof. A. Reller, Hamburg, for generous support. This work was financially supported by the Deutsche Forschungsgemeinschaft (Bonn, Germany) and the Fonds der Chemischen Industrie (Frankfurt/Main, Germany). J.M.T. thanks the Engineering and Physical Sciences Research Council (EPSRC, U.K.) for a rolling grant and allocation of synchrotron beam time at the CCLRC Daresbury laboratory. We are grateful to O. Herzberg, Hamburg, for preparing the sodium bromoacetate sample and some electron microscopic experiments.

CM9704138

(52) Bunker, G. *Nucl. Instrum. Methods* **1983**, *207*, 437.

(53) Frenkel, A. I.; Rehr, J. J. *Phys. Rev. B* **1993**, *48*, 585.

(54) Frenkel, A. I.; Stern, E. A.; Qian, M.; Newville, M. *Phys. Rev. B* **1993**, *48*, 12449.